 doi:10.20944/preprints202006.0326.v1

Investigating Potential Inhibitory Effect of *Uncaria tomentosa* (Cat`s claw) against the Main Protease 3CL^{Pro} of SARS-CoV-2 by Molecular Modeling

Andres F. Yepes-Pérez [1], Oscar Herrera-Calderon [2*], José-Emilio Sánchez-Aparicio[3], Laura Tiessler-Sala[3], Jean-Didier Maréchal [3*] and Wilson Cardona-G[1]

1. Chemistry of Colombian Plants, Institute of Chemistry, Faculty of Exact and Natural Sciences University of Antioquia-UdeA, Calle 70 No. 52-21, A.A 1226, Medellin, Colombia; andresf.yepes@udea.edu.co (A.F.Y.-P.); wilson.cardona1@udea.edu.co (W.C.G.).

2. Academic Department of Pharmacology, Bromatology and Toxicology, Faculty of Pharmacy and Biochemistry, Universidad Nacional Mayor de San Marcos, Jr Puno 1002. Lima 15001, Peru; oherreraca@unmsm.edu.pe (O.H.-C.)

3. Insilichem, Departament de Química, Universitat Autònoma de Barcelona, Edifici C.n., 08193 Cerdanyola del Vallés, Barcelona, Spain; JeanDidier.Marechal@uab.cat (J.-D.M.); laura.tiessler@uab.cat (L.T.S.); joseemilio.sanchez@uab.cat (J.-E.S.-A.).

* Correspondence: oherreraca@unmsm.edu.pe (O.H.-C.)

Preprints (www.preprints.org) | NOT PEER-REVIEWED | Posted: 28 June 2020 doi:10.20944/preprints202006.0326.v1

Investigating Potential Inhibitory Effect of *Uncaria tomentosa* (Cat`s claw) against the Main Protease 3CL^{Pro} of SARS-CoV-2 by Molecular Modeling

Abstract

COVID-19 is a novel severe acute respiratory syndrome coronavirus. Presently, there is no effective treatment for COVID-19. As part of the worldwide efforts to find efficient therapies and preventions, it has been reported the crystalline structure of the SARS-CoV-2 main protease Mpro (also called 3CL^{pro}) bound to a synthetic inhibitor which represents a major druggable target. The druggability of M^{pro} could be used for discovering drugs to treat coronavirus disease 2019.

It was carried out a multi-level computational study to evaluate the potential anti-viral properties of the components of the medicinal herb Uncaria tomentosa (Cat´s claw) focusing on the inhibition of Mpro. The in-silico approach starts with protein-ligand docking of 26 Cat's claw key components followed by ligand pathway calculations, molecular dynamics simulations and MM-GBSA calculation of the free energy of binding for the best docked candidates.

The structural bioinformatics approaches led to the identification of three bioactive compounds of Uncaria tomentosa (Speciophylline, Cadambine and Proanthocyanidin B2) with potential therapeutic effects by strong interaction with 3CLpro. Additionally, in silico drug-likeness indices for these components were calculated and show good predicted therapeutic profiles of these phytochemicals.

Our findings suggest the potential effectiveness of Cat's claw as complementary and/or alternative medicine for COVID-19 treatment.

Keywords: SARS-CoV-2; 3CL^{pro} protein; Cat's Claw; *Uncaria tomentosa*; Molecular Modeling.

 doi:10.20944/preprints202006.0326.v1

1. Introduction

The 2019 novel coronavirus (2019-nCoV) known also as the severe acute respiratory syndrome corona virus 2 (SARS-CoV-2) is a part of Coronavirus Family (CoV) and was initially identified in Wuhan, China at the end of December 2019 . COVID-19 is highly contagious and is most frequently transmitted from human to human, spreading the virus easily to other countries in a very short time. According to the last report of the World Health Organization (WHO), 2019-nCoV, which causes the severe acute respiratory syndrome (coronavirus disease COVID-19) is considered a pandemic, affecting Asia and Europe with the highest death rate followed by America and other regions, causing serious problems of public health and considerable economic losses worldwide [2]. Respiratory viral infections are the frequent causes of morbidity and millions of hospital admissions in developing countries every year [3]. For this reason, the pharmacotherapy based on natural products may be a proper alternative for treating viral diseases. On the other hand, traditional medicine is practiced in native South American inhabitants whose know the medicinal properties of many plants from the rainforest [4]. Therefore, many of them are collected by ethnobotanists who investigate their resources as antimicrobial [5], antitumor agents [6] and being the main source for target selection during scientific investigation on compounds with antiviral activity [7]. The biodiversity of South America countries offers a series of medicinal plants and could combat the symptoms of infections such as coronavirus disease COVID-19.

Uncaria tomentosa (Willd. ex Schult.) DC. named Cat's claw ("uña de gato" in Spanish) is a woody vine indigenous to the Peruvian Amazon and other tropical areas of South and Central America that belongs to Rubiaceae family [8, 9, 10]. In Peru, natives from the villages in the region of Chanchamayo and Nevati near Puerto Bermudez, Junin, boiling approximately 20 g of sliced root bark in 1 liter of water for 45 min commonly used in religious purposes and curatives [11]. This species is marketed as dry and ground material remarkably in recent years, being widely studied in all aspects mainly chemical (isolated chemical structures) and bioassays *in silico, vitro, in vivo* and some medical trials. Currently, the raw material of *U. tomentosa* is dispensed in Public Hospitals of the Social Health

 doi:10.20944/preprints202006.0326.v1

Insurance (EsSalud-Peru) as Complementary Medicine Service (CMS) [12]. Traditionally, extracts prepared by roots and barks decoction are used against several diseases, such as allergies, arthritis, inflammations, rheumatism infections and cancer [13]. However, its popular use has been widely known in worldwide and analytical tests can be found in the United States Pharmacopeia (USP) and dosage forms have been only authorized as Dietary Supplements.

Bioactive constituents of *U. tomentosa* extracts include proanthocyanidins (proanthocyanidin B2, the main component; proanthocyanidin B4, proanthocyanidin C1, an epicatechin trimer, epiafzelechin-4β→8-epicatechin and an epicatechin tetramer) [14], oxindole alkaloids (isopteropodine, pteropodine, rhynchophylline, mytraphylline, speciophylline, uncarine F and uncarine E), indole alkaloidal glucosides (cadambine, 3-dihydrocadambine, and 3-isodihydrocadambine), quinovic acid glycosides, tannins, polyphenols, catechins, beta sitosterol and proteins which individually or synergistically contribute to their therapeutic properties [15].

In regards to its antiviral properties of *U. tomentosa*, the alkaloid fraction has demonstrated to be the most effective on human monocytes infected with Dengue Virus-2 (DENV) *in vitro* [16]. Another study revealed that only the alkaloidal fraction has inhibitory activity on Dengue Virus and negative effect was observed with the non-alkaloidal fraction [17]. In another study, the antiherpetic activity from *U. tomentosa* seems to be associated with polyphenols or with their synergistic effect with pentacyclic oxindole alkaloids or quinovic acid glycosides [18]. *U. tomentosa* hydroethanolic extracts demonstrated a significant *in vitro* inhibitory effect on the replication of herpes simplex virus type 1 and the inhibition of viral attachment in the host cells was characterized as the main mechanism of its antiviral activity [19]. Furthermore, other investigations mentioned immunomodulating activity which includes, stimulation of phagocytosis, enhancement of B- and T-lymphocytes, suppression of NF-kappa B, enhancement of IL-1 and IL-6 [20]. In a Peruvian study on rats, the investigators found that phagocytosis was increased and might act as potent inhibitor of TNF-α [21]. In 2008, a study evidenced a possible drug-drug interaction between Cat's claw and protease inhibitors such as saquinavir, atazanavir and ritonavir, increasing level of

 doi:10.20944/preprints202006.0326.v1

these drugs in plasma [22]. Individuals supplemented with a novel water-soluble extract of *Uncaria tomentosa*, (C-Med-100®) increased effectiveness of pneumococcal vaccination by an elevation in the lymphocyte/neutrophil ratios of peripheral blood and a reduced decay in the 12 serotype antibody titer responses to pneumococcal vaccination [23].

With neither drugs nor vaccines approved against 2019-nCoV yet, finding strategies to diminish the impact of the pandemic is fundamental. Medicinal herbs and, more particularly, those with demonstrated anti-viral activities are possible allies in this quest. Their use could slow down the spreading of the disease. Particularly in developing countries, in which the accessibility to these plants is easier and more economically viable, adding these medicinal herbs to the general medical kit may be beneficial. In addition, traditional knowledge of these remedies may reduce possible side effects, allowing them to be implemented with fewer medical risks. [24].

On the basis of the aforementioned background of *Uncaria tomentosa* (Cat`s claw), this work aims at computationally identifying potential bioactive compounds against COVID-19. It focuses on possible interactions and inhibition of the $3CL^{pro}$ protease (also called M^{pro}). $3CL^{Pro}$ is responsible of 100% of proteolytic mechanism of the virus and is involved in virulence, infectivity, transcription and replication cycle of the virus [25-26]. It has been identified as the main druggable target of SARS-Cov-2 for new antiviral discovery. Moreover, its X-ray structure has been recently released hence allowing possible computational analysis [2]. In fact, several computational studies have already been undertaken on this system including a long 20μs molecular dynamics (MD) study and virtual screening of several databases [27].

Here, our study stands on a multi-level computational strategy reminiscent to those applied at the early stage of current state-of-the-art drug discovery pipelines and includes 1) protein-ligand docking of all bioactive compounds of Cat's claw against $3CL^{pro}$ structure, 2) simulations of ligand pathway of the best predicted compounds from step 1 to evaluate convenient entrance mechanism of the compounds to the binding site, 3) molecular dynamics simulation to assess the stability of the best protein-ligand complexes from 2, 4) calculation of the free energy of binding based on MD post-processing (MM-GBSA) and 5)

Preprints (www.preprints.org) | NOT PEER-REVIEWED | Posted: 28 June 2020 doi:10.20944/preprints202006.0326.v1

calculation of pharmacokinetics parameters for the most qualified compounds resulting from the previous parts of the protocol. The study leads to the identification of at least two compounds with potential anti-viral activity in Cat's claw-based products to aim propose ethanolic extract of *Uncaria tomentosa* as rapid phytotherapeutically option for COVID-19.

2. Materials and Methods

2.1. Protein Structure and Setup

Calculated binding affinity of the main constituents of the Cat´s claw extracts (Table 1) was explored against the main protease $3CL^{Pro}$ of 2019-nCoV findings a facile therapeutic option for anti-coronaviral therapy, the crystal structure of protease $3CL^{Pro}$ were downloaded from the Protein Data Bank (PDB entry code 6LU7) [28] and all bounded ligands, ions and solvent molecules were manually removed using the DS Visualizer 2.5 program. For docking studies, the structure of the selected protein was parameterized using AutoDock Tools [28]. Gasteiger partial charges were calculated and polar hydrogens to facilitate the formation of hydrogen bonds were added.

2.2. Ligand dataset preparation and optimization

Ligands used in this study are major components of the Cat´s claw extracts, a potent irreversible inhibitor recently reported for COVID-19 virus $3CL^{pro}$ (namely N3) [28] and three well-known FDA approved viral protease inhibitors that may be repurposed to treat Covid-19 [29-34]. The 2D structures of the 26 Cat´s claw constituents were obtained as mol.2 files from the ZINC database [35]. The resultant compounds were submitted to MarvinSketch 8.3 [36] to correct the protonation states of the ligands at physiological pH 7.4 and its structures parameterized using AutodockTools to add full hydrogens to the ligands, to assign rotatable bonds, to compute Gasteiger charges and saving the resulting structure in the required format for use with AutoDock. All possible flexible torsions of the ligand molecules were defined using AUTOTORS in PDBAutoDockTools [28,37] to promote the calculated binding with the 2019-nCoV protease structure.

Preprints (www.preprints.org) | NOT PEER-REVIEWED | Posted: 28 June 2020 doi:10.20944/preprints202006.0326.v1

2.3. *Docking-based virtual screening*

Our docking protocol were performed using AutoDock 4.2 with the Lamarkian genetic algorithm and default procedures to dock a flexible ligand to a rigid protein. Docking simulation was carried out on the main protease $3CL^{Pro}$ of 2019-nCoV cleavage site (PDB code: 6LU7), where the enzyme residues are in close proximity to the recently reported potent inhibitor, known as N3, which was co-crystallized in complex with the main 2019-nCoV protease. Once a potential binding site was identified, 26 compounds which are the major components of the Cat´s claw extracts were docked to this enzyme-site to determine the most probable and the most energetically favorable binding conformations. To accomplish that, rigorous docking simulations involving a grid box to the identified catalytic site, Autodock Vina 1.1.2 [38] was used. The exhaustiveness was 20 for each protein-ligand pair (number of internal independent runs). The active site was surrounded by a docking grid of 42 $Å^3$ with a grid spacing of 0.375 Å. Affinity scores (in Kcal/mol) given by AutoDock Vina for all compounds were obtained and ranked based on the free energy binding theory (more negative value means greater binding affinity). The resulting structures and the binding docking poses were graphically inspected to check the interactions using the DS Visualizer 2.5 (http://3dsbiovia.com/products/) or The PyMOL Molecular Graphics System 2.0 programs.

2.4. *GPathFinder calculations*

To assess the feasibility of the binding route for the ligand, ten runs of GPathFinder [37] calculations for each ligand-protease complex were performed. The ligand was placed at the position obtained from docking calculations and required to search for a possible unbinding route to outside the protease. Full flexibility was allowed for the ligand along the pathway including rotameric states of amino acid side chain and backbone motions based on some previous MD simulations of 10μs. A clustering was carried out by means of the quality threshold methodology [39] to obtain a pool of 110 representative frames from a 10

Preprints (www.preprints.org) | NOT PEER-REVIEWED | Posted: 28 June 2020 doi:10.20944/preprints202006.0326.v1

μs simulation of the apo structure [38]. This pool of representative frames was used as the possible conformations that the protease could adopt during the ligand transport. Vina score and steric clashes were minimized to obtain a total of 120 solutions for each run. A complete input file to use with version 1.2.1 of the software is provided in Supplementary Materials.

2.5. Molecular dynamics simulations

All the Molecular Dynamics (MD) simulations were carried out using the dimeric structure of COVID main protease available in the PDB [40] (code 6lu7) as receptor. The best-scored docking positions were used as starting conformations for the ligands. Two ligands (one for each monomer) were placed at symmetric positions of the dimeric structure. The protein was prepared by removing waters and crystallographic small molecules from the PDB structure to have the protease residues free of interact with the ligands during the simulation. Finally, protons were then added through the algorithm implemented in UCSF Chimera Software [41].

MD simulations were set up with the LEaP, which was instructed to solvate the protein with a cubic box of pre-equilibrated TIP3P water molecules and balance the total charge with Na+ ions (ions94.lib library). The AMBER14SB force field [42] was used for the standard residues, while the GAFF force field was adopted for the remaining atoms. The geometries of the ligands were optimized in water solvent (SMD continuum model) at DFT level of theory using Gaussian09 [42]. Geometry and frequency calculations were performed using the B3LYP hybrid functional with 6-31G(d,p) as basis set and included Grimme's dispersion. Atomic charges were computed using the RESP protocol [43] (restrained electrostatic potential) at the same level of theory and the atom types and force constants and equilibrium parameters were assigned using antechamber and parmchk2 from AmberTools18 [44].

For all the MDs, the solvent and the whole system were sequentially submitted to 3000 energy minimization steps to relax possible steric clashes. Then, thermalization of the system was achieved by increasing the temperature from 100 K up to 300 K. MD simulations

Preprints (www.preprints.org) | NOT PEER-REVIEWED | Posted: 28 June 2020 doi:10.20944/preprints202006.0326.v1

under periodic boundary conditions were carried out for 250ns with OpenMM engine [39] using the OMMProtocol [45]. Three simulations were run in total, considering the following protease-ligand systems: Speciophylline, Cadambine and Proanthocyanidin B2.

Analysis of the trajectories was carried out by means of CPPTraj implemented in AmberTools18. The MD trajectory was considered converged when a stable exploration of the conformational space was achieved. In particular, a stable conformation or a pool of relative stable conformations visited for a statistically consistent number of times were considered as convergence indicators [46, 47]. Considering the alpha carbons of the protease backbone, RMSD from the minimized structure, all-to-all frames RMSD and cluster counting analysis were performed. Moreover, to ensure that dynamic transitions occur between different conformations, a Principal Component Analysis (PCA) was carried out plotting the two principal modes relative to each other.

The distance from the geometric center of the ligand to the center of the binding site was computed along all the trajectories. Alpha carbons of residues GLY143, CYS145, HIS163, HIS164, GLU166, GLN189 and THR190 were considered to calculate the center of the binding site, and the distance from the crystallographic inhibitor N3 to that binding site center (3.947 Å) was taken as reference for comparison.

2.6. Prediction of drug-likeness properties for the most docking promissory compounds

Drug-likeness prediction along with further ADME properties present a wide of opportunities for a rapid new antiviral drug discovery. The drug-like and ADME properties for the most active components of the Cat´s claw extracts (constituents having the highest binding affinity) were screened using open-access cheminformatics platforms such as Molinspiration (for molecular weight-MW, rotatable bonds and polar surface area-PSA descriptors), ALOGPS 2.1 (for Log $P_{o/w}$ descriptor) and the Pre-ADMET 2.0 to predicted four pharmaceutical relevant properties such as intestinal permeability (App. Caco-2), albumin-binding proteins (K_{HSA}), Madin-Darby Canine Kidney (MDCK Line) cells permeation and intestinal absorption (%HIA). These parameters establish movement, permeability,

Preprints (www.preprints.org) | NOT PEER-REVIEWED | Posted: 28 June 2020 doi:10.20944/preprints202006.0326.v1

absorption and action of potential drugs. The interpretation of both MDCK and Caco-2 permeability using PreADMET as follows:

1. Permeability lower than 25: low permeability.
2. Permeability between 25 and 500: medium permeability.
3. Permeability higher 500: high permeability.

3. Results and discussion

3.1. Database of Cat's claw bioactive compounds.

This study was performed to identify if certain components of Cat´s claw extracts may have potential therapeutic effects against COVID-19. To do so, a database of 26 compounds that have shown prevalence on the herb therapeutic activity has been generated (Figure 1) [14, 15]. Our initial hypothesis is that Cat's claw should contain molecules with highest therapeutic profiles against 2019-nCov, by its interaction with $3CL^{Pro}$ main protease.

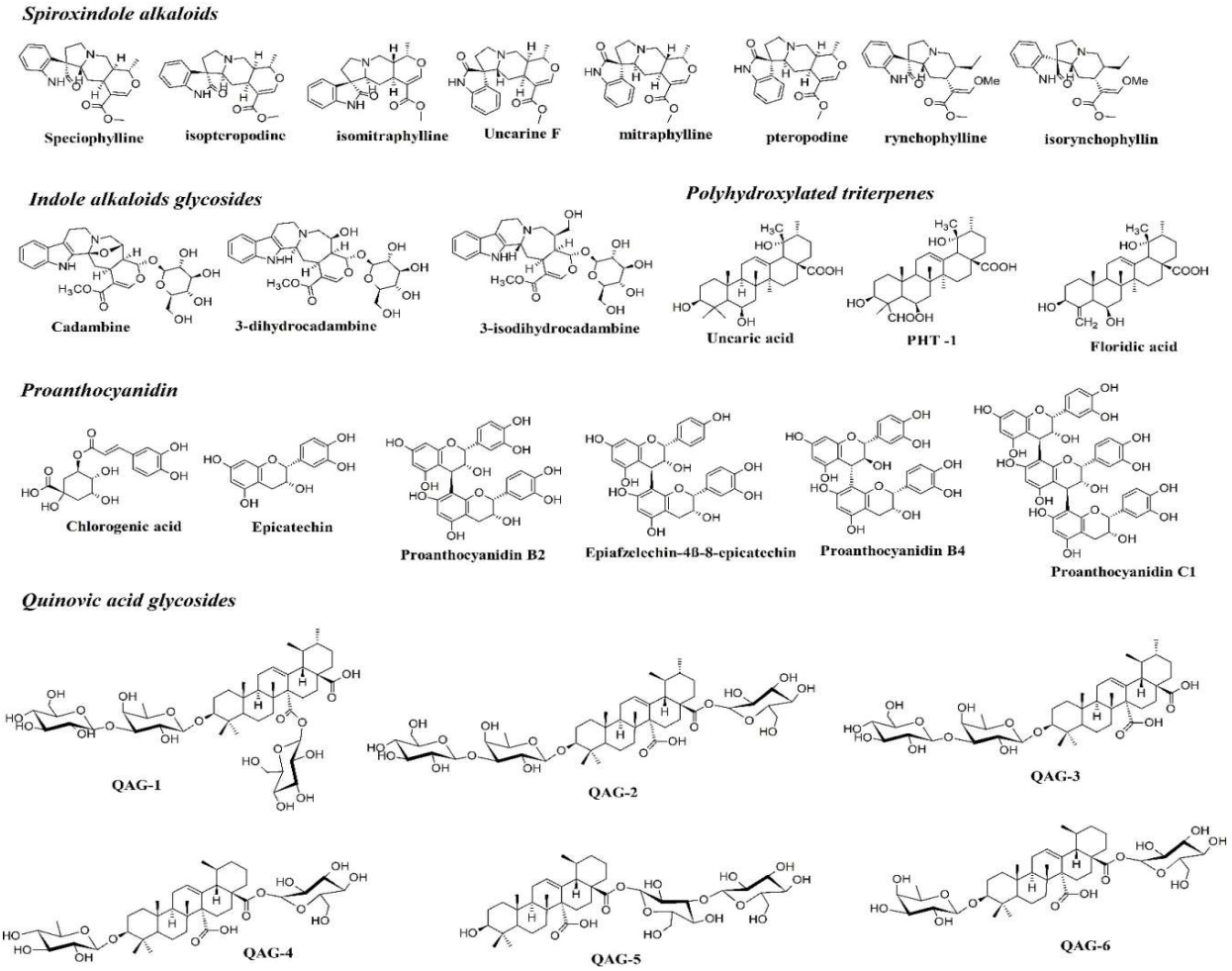

 doi:10.20944/preprints202006.0326.v1

Figure 1. 2D-structures for the major bioactive constituents of the Cat´s claw studied as ligands against the novel 2019-nCoV main protease.

3.2. Docking results

Despite limitations in term of energetic functions (scoring) and conformational sampling (limited to ligand rotational bound mainly and restricted local motion of the protein at the most), protein-ligand dockings are still today the main computational strategy to identify potential binders to a given protein target. Protein-ligand dockings of the 26 constituents of Cat´s claw were performed against the three-dimensional structure of 2019-nCoV main protease $3CL^{pro}$ (PDB: 6LU7) [28] to aim study the potential of ethanolic extract of Cat´s claw for COVID-19 treatment based on its majority components.

The structure of $3CL^{pro}$ shows the protein to be a homodimer with subunit 306 amino acids long (figure 2). The catalytic site is mainly constituted by loops and hairpins that suggests a flexible site; a feature common in many proteases. The co-crystallized N3 drug stands in the catalytic site that defines the cleavage S1 subsites and are characterized by the following amino acids: THR190, GLN189, GLU166, HIS164, CYS145, GLY143, GLU166, HIS163, PHE140, ASN142, MET49, HIS41, MET165, ARG188 and ASP187.

This site was defined as the binding pocket for the docking runs. Because of the symmetry in the X-ray structure between the two dimers of the $3CL^{pro}$, dockings were performed on only one monomer. Molecular docking studies were performed with Autodock for all compounds.

Preprints (www.preprints.org) | NOT PEER-REVIEWED | Posted: 28 June 2020 doi:10.20944/preprints202006.0326.v1

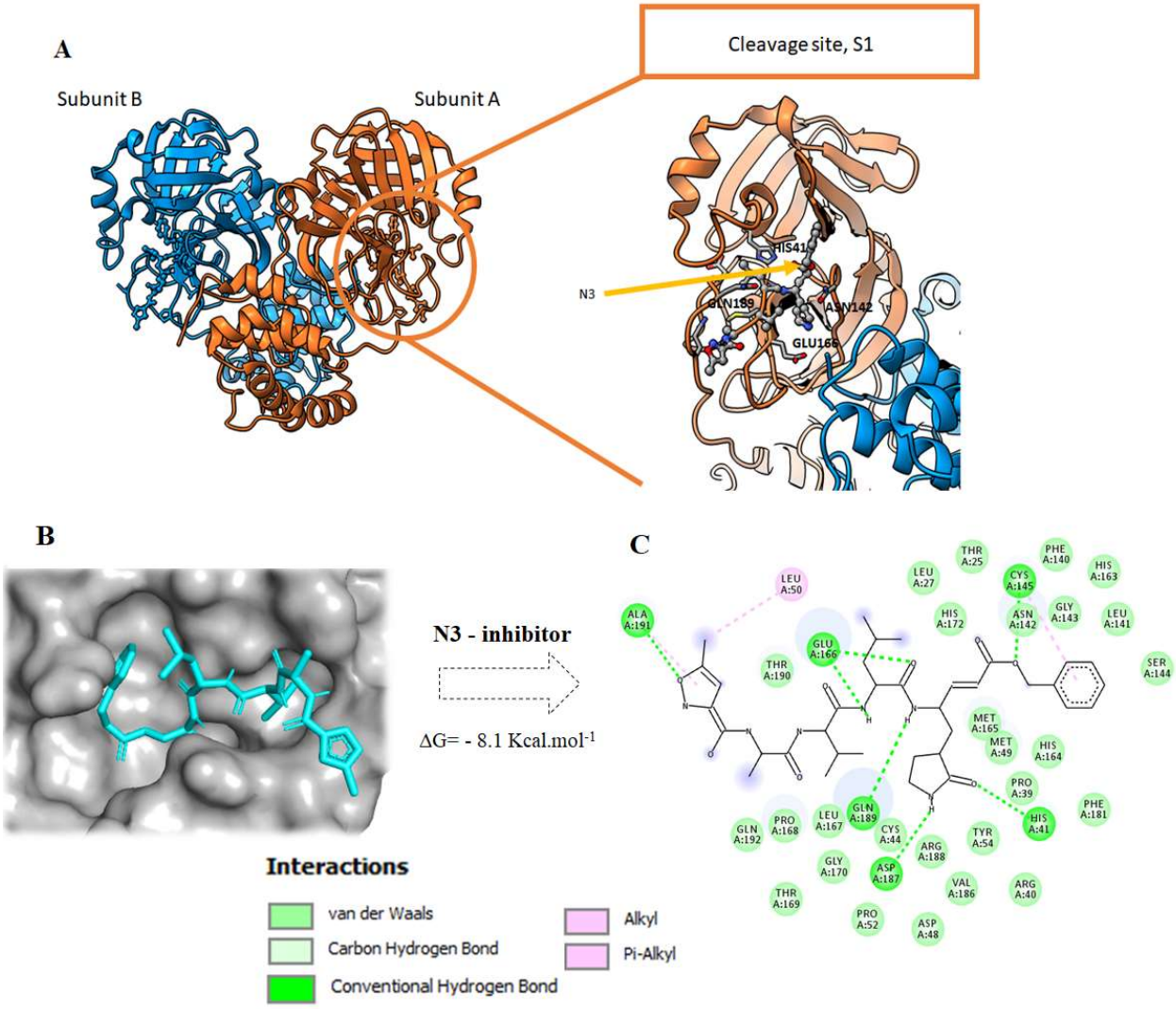

Figure 2. (A) Representation of the 3CL^{pro} protease with N3 inhibitor bound. Overall structure of the dimer (left) and cleavage site S1. (B) The best conformation of the potent 3CL^{Pro} inhibitor N3 into 3CL^{pro} (C) 2D ligand-protease interaction plot between the inhibitor N3 with 3CL^{pro}. Dashed lines indicate interactions of N3 with 3CL^{pro}.

All compounds show docked structures that fit well into the S1 cavity of 3CL^{pro} (Figure 3A-B) and with good predicted docking scores that range from -5.9 to -9.2 kcal/mol (Table 1 and figure S1). In general, calculations revealed that most of the 12 amino acids involved in the N3-3CL^{Pro} interactions identified in the X-ray structures also constitute the binding pocket of the docking solutions. In particular, most predicted complexes have the interaction fingerprint with CYS145, GLU166, MET165, GLN189 and GLY143; the most important residues in the reported active pocket for 2019-nCoV (figure 3B-C).

Preprints (www.preprints.org) | NOT PEER-REVIEWED | Posted: 28 June 2020 doi:10.20944/preprints202006.0326.v1

Importantly, some compounds have similar or even lower binding free energies values than those of N3 and other FDA-approved viral protease inhibitors identified as $3CL^{pro}$ binders which have energies ranging from -8.0 to -8.5 kcal/mol (see the references section of table 1). At this point it is worth mentioning that the docking calculations involving these drugs give values in very good agreement with experimental ones and round the -8.1 kcal/mol hence providing with a certain amount of confidence regarding the Autodock scoring function of this project.

Table 1. Best binding energy (kcal/mol) based on AutoDock scoring of the main constituents of the Cat´s claw into the cleavage site of the novel 2019-nCoV main protease (PDB ID: 6LU7).

Main constituents of Cat´s claw	Best binding energy (kcal/mol)	Main constituents of Cat´s claw	Best binding energy (kcal/mol)
Spiroxindole alkaloids		**Quinovic acid glycosides**	
Speciophylline	-8.1	QAG-1	-7.8
Isopteropodine	-6.6	QAG-2	-7.4
Isomitraphylline	-7.6	QAG-3	-7.2
Uncarine F	-8.2	QAG-4	-7.9
Mitraphylline	-7.0	QAG-5	-7.8
Pteropodine	-7.0	QAG-6	-7.8
Rynchophylline	-5.9	**Proanthocyanidins**	
Isorynchophyllin	-6.1	Chlorogenic acid	-6.8
Indole glycosides alkaloids		Epicatechin	-7.2
Cadambine	-8.6	Proanthocyanidin B2	-9.2
3-dihydrocadambine	-8.0	Epiafzelechin-4β-8-Epicatechin	-8.9
3-isodihydrocadambine	-8.0	Proanthocyanidin B4	-9.2
Polyhydroxylated triterpenes		Proanthocyanidin C1	-8.8
PHT -1	-6.8	**References**	
Uncaric acid	-7.0	N3 [a]	-8.1 (-8.1) [b] (-8.3) [c] (-7.9) [d]
Floridic acid	-7.6	Remdesivir [h]	-8.5
		Ritonavir [h]	-8.1 (-7.7) [e] (-7.5) [f] (-8.9) [g]
		Lopinavir [h]	-8.0 (-8.4) [e] (-7.4) [f] (-9.4) [g]

[a] potent irreversible inhibitor of COVID-19 virus $3CL^{pro}$. [b] binding affinity reported by Haider et al [48]. [c] binding affinity reported by Khaerunnisa *et al* [49]. [d] binding affinity reported by Chauhan [50]. [e] binding affinity reported by Kaifu et al [51]. [f] binding affinity reported by Talluri [52]. [g] binding affinity reported by Chen et al [53]. [h] FDA approved antivirals drugs promising to treat COVID-19. [30-33].

Notably nine components have calculated affinities that range from -8.1 to -9.2 $Kcal.mol^{-1}$. In this set of nine molecules, we found that most of the proanthocyanidins of Cat's claw extract show the higher binding affinities to $3CL^{pro}$ with regard to any other

Preprints (www.preprints.org) | NOT PEER-REVIEWED | Posted: 28 June 2020 doi:10.20944/preprints202006.0326.v1

family of compounds. This result is consistent with several *in vitro* and *in vivo* studies that show that proanthocyanidins display potent virucidal activity for herpes simplex virus (HSV), human immunodeficiency virus (HIV), influenza A and B, hepatitis B and D, Human Norovirus and Aichi virus (AiV), respectively [55-60]. The five remaining compounds of high affinity for $3CL^{pro}$ are from the two alkaloidal fractions, the Spiroxindole and the Indole glycosides ones. These findings are also consistent with previous reports demonstrating the antiviral properties of the alkaloid fractions from Cat´s claw [17-19]. Amongst those compounds speciophylline and cadambine are particularly interesting since they are part of the phytochemical fingerprint for *Uncaria tomentosa* (Cat's claw).

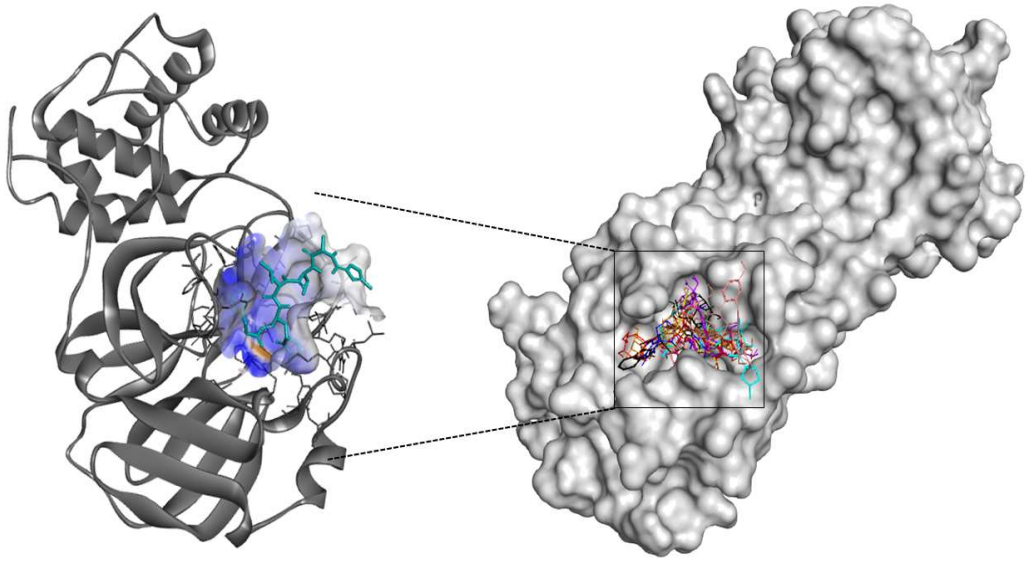

Figure 3. (A) N3 into $3CL^{pro}$ cleavage pocket (B) Superposition of the best conformation of the most active components Speciophylline (in yellow), Uncarine F (in blue), Cadambine (in red), 3-dihydrocadambine (in orange), 3-isodihydrocadambine (in black), Proanthocyanidin B2 (in purple), Epiafzelechin-4β-8-epicatechin (in brown), Proanthocyanidin B4 (in magenta), and N3 (in cyan) a potent $3CL^{pro}$ inhibitor.

From this part of the study, nine components are computationally estimated to have similar or even better binding affinities for the $3CL^{pro}$ cleavage site S1 than the current protease inhibitor N3 and other antiviral drugs. Speciophylline, Cadambine and Proanthocyanidin B2 were selected for further investigation since they are of the best representative of three different families of compounds of the Cat's claw fractions (docking scores of -8.1, -8.6 and -9.2 kcal/mol, respectively).

Preprints (www.preprints.org) | NOT PEER-REVIEWED | Posted: 28 June 2020 doi:10.20944/preprints202006.0326.v1

3.3. *Ligand Pathway analysis.*

A first series of refinements consisted in the simulation of the ligand pathways of Speciophylline, Cadambine and Proanthocyanidin B2 to the catalytic site S1 of $3CL^{pro}$. Indeed, protein-ligand docking does not account with the protein motions associated to the transition of the ligands from solvent to the binding site; a phenomenon that could lead to false positives in screening steps of drug discovery processes and to avoid for further stages. To ascertain the accessibility of the compounds to the cleavage site, calculations were undergone using the GPathFinder software [60]. For each compound 120 channels were calculated (10 runs segmented in finding the 12 lowest energy paths), and their results averaged. The sampling of the protein structure was based on 110 snapshots from the 10µs simulation of the unbound structure recently released [61] hence allowing that large scale motions (domain motions) could be accounted in the simulation.

For the three compounds, the calculations tend to converge to the same entrance pathway that mainly involve rearrangements of the loop and hairpin motives that constitute the S1 cleavage site as well as some breathing motions involving the alpha helix domain of the dimer (figure 4). For all ligands, low energy barriers are observed and none overcome the 5.3 kcal/mol in average (± 3.2 kcal/mol) (see table S1). This value is consistent with the relatively solvent exposed binding site of the protease and suggests the absence of restrictive motions for the binding of the ligands. It was noticed that the lowest barrier is observed for speciophylline with a value of 2.4 kcal/mol.

Preprints (www.preprints.org) | NOT PEER-REVIEWED | Posted: 28 June 2020 doi:10.20944/preprints202006.0326.v1

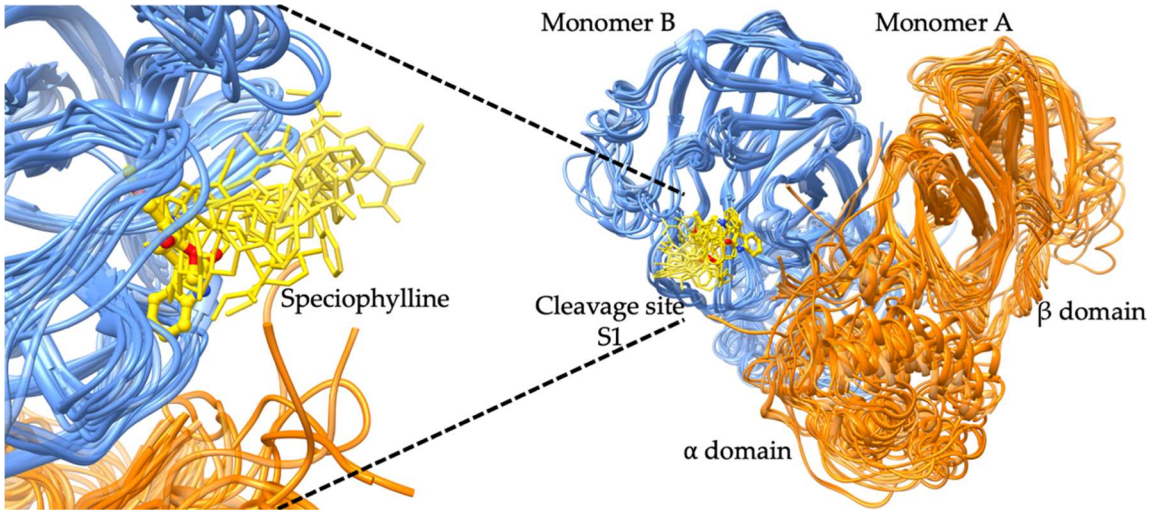

Figure 4. Schematic view of the entrance pathway for Speciophylline into the monomer B of $3CL^{pro}$ protease of SARS_nCov19. The ligand is colored in yellow and the protein in orange (monomer A) and blue (monomer B). Snapshots of the lowest energy pathway are presented with the ligand represented in thin sticks and the final pose in ball and stick.

To this point, our study shows that Speciophylline, Cadambine, and Proanthocyanidin B2 have: 1) good predicted binding affinity for S1 cleavage site and 2) they can naturally access it without noticeable energetical cost.

3.4. Molecular dynamics (MD) simulations and calculations of the free energy of binding

With higher confidence on the viability of our docking predictions for Speciophylline, Cadambine, and Proanthocyanidin B2, we further evaluated the stability of the docked complexes throughout molecular dynamics simulations. Calculations were performed with openMM software [62] and the Amber force field [63] (for details readers can refer to material and methods). It is important to notice that the simulations were carried out on the dimeric (hence complete) structure of the protease-ligand complexes after their reconstruction by symmetric operation. For each system then the stoichiometry ligand:protein is 2:1 (2 ligands for one dimer).

We assessed the quality of our MD experiment by using four different criteria: 1) root mean square deviation of the backbone (RMSD), 2) all-to-all RMSD, 3) principal component analysis (PCA) and 4) cluster counting. This combination of analytical tools has previously proven to be a reliable assessment methodology of protein structural convergence [65,66].

Preprints (www.preprints.org) | NOT PEER-REVIEWED | Posted: 28 June 2020 doi:10.20944/preprints202006.0326.v1

Moreover, ligand and protein flexibility were assessed by calculation of RMSF analysis. By taking all these parameters into account, all simulations were run until 250ns each (see figure 5 for Speciophylline as an illustrative case of analysis and ESI figures S3 and S4 for Cadambine and Proanthocyanidin B2).

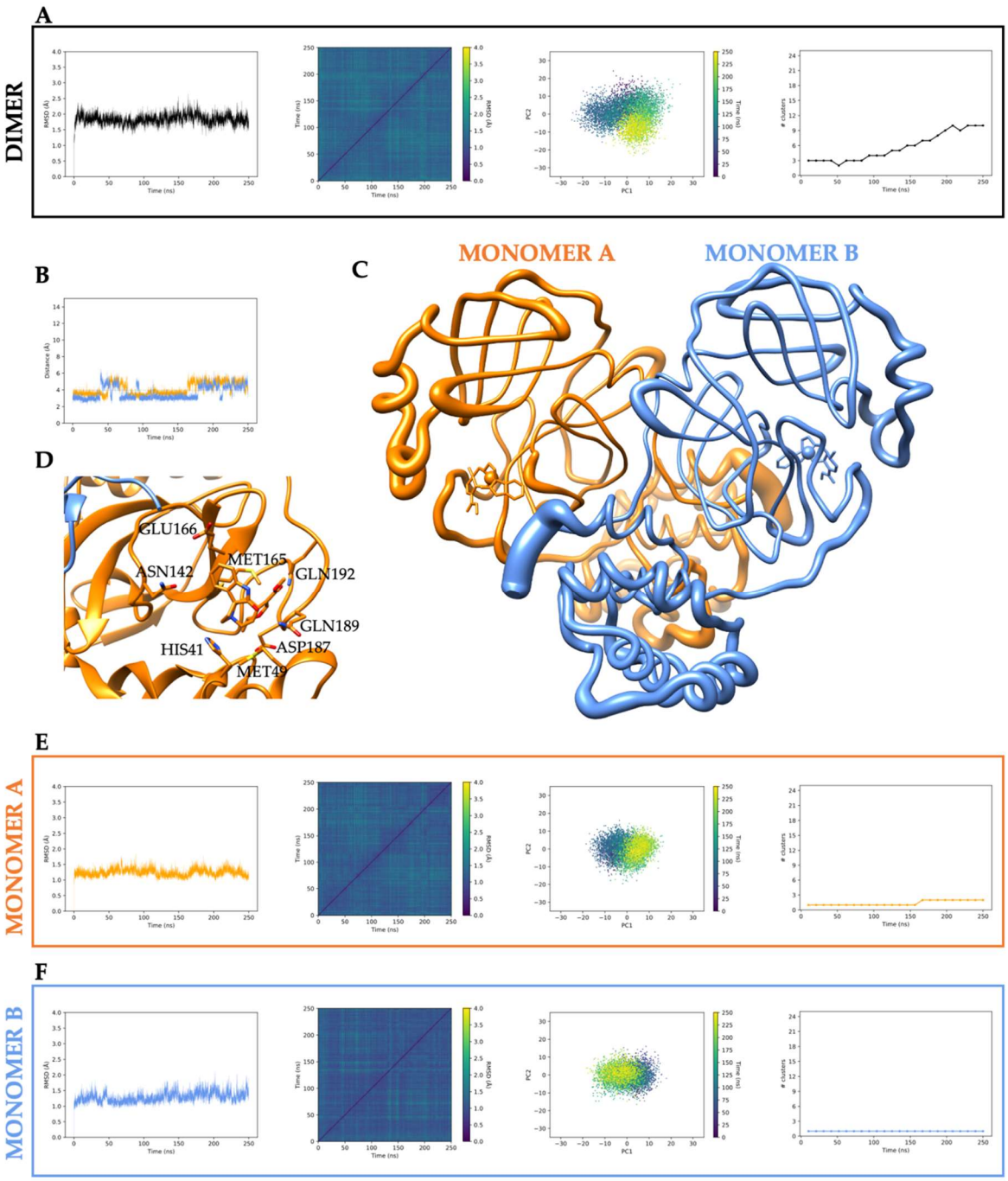

Preprints (www.preprints.org) | NOT PEER-REVIEWED | Posted: 28 June 2020 doi:10.20944/preprints202006.0326.v1

Figure 5. Complete analysis of the 250ns trajectory of $3CL^{pro}$ of SARS-nCov19 bound with Speciophilline. Orange color reports to the monomer A and blue to monomer B. Panels A, E and F, contains, from left to right: RMSD, all-to-all RMSD, PCA and cluster counting (cutoff 1,5Å). Panel B shows the relative position of Speciophylline molecules versus the center of mass of the S1 cavity along the simulation (black dashed line indicates the distance of N3 inhibitor as reference). For panel C, size of the ribbon is proportional to the flexibility of the protein backbone and the size on the ligand center is proportional to the amount of structural deviation of the ligand during the 250ns. Panel D reproduces the binding site S1 with the most important residues involved in the interactions.

Based on the analysis of these different variables and visual inspection, a clear behavior appears along the molecular dynamics that summarizes as follows:

1) The overall trajectories of all systems are stable with no modification in terms of the secondary structure. Only slight transitions on the tertiary structure (intra and intermonomeric interfaces) are observed though of different magnitudes depending on which Cat's claw component is bound and their motion during the course of the MD.

2) For Speciophylline, both monomers behave in a very symmetric manner with the ligands remaining well sited into the cavity the entire course of the simulation and at the same location of the initial docking solution (Figure 5.B and 5.C). However, two different orientations are observed. The orientation with higher time of residence is very close to the initial docked complex with most of the interactions of the cleavage site maintained though additional hydrogen bonds that appear with Gln189 and Gln192 (figure 5.D, table S2). The second one shows Speciophylline displaying a slight rotation around its main axis of inertia (figure 5.B). This second orientation appears related to the loss of the hydrogen bond of the Gln189 as well as a slight rearrangement of the α domain with respect to the β domain. These changes in the ternary structure are also related to modifications of the interfaces between both monomers. It is to note that those motions are consistent with those observed for ligand binding simulation of the previous GPathFinder calculations (see previous section and figure 4).

3) For Cadambine and Proanthocyanidin B2, the overall fold is also very stable. However, a conformational change occurs at about 200ns that essentially affects the tertiary and quaternary nature of the system (Figure S3 and S4). Further inspection shows that both monomers have also distinct behaviors. While the ligand remains in monomer B all along the simulation with poses close to the predicted docked complex and strong interaction with

Preprints (www.preprints.org) | NOT PEER-REVIEWED | Posted: 28 June 2020 doi:10.20944/preprints202006.0326.v1

the catalytic binding site, monomer A displaces its ligand at about 200ns which then remains closer to the entrance of the monomer binding site. This displacement toward more solvent exposed location of monomer A is more pronounced for Proanthocyanidin B2 than Cadambine (Figure S3 and S4). Therefore, Cadambine and Proanthocyanidin B2 seem to lead to one very stable binding with associated conformational changes that relate, in an apparent allosteric manner, on the second one.

These structural observations were further quantified by MM-GBSA analysis (table 2). Results show the $\Delta G_{binding}$ of the species in the different monomer range from ca. -52 kcal/mol to ca. -15 kcal/mol. Taking average values between $S1_A$ and $S1_B$ sites, the affinity of the different phytochemical compounds to $3CL^{Pro}$ can be classified as Cadambine (aprox. -40kcal/mol) > Speciophylline (aprox. -35 kcal/mol) > Proanthocyanidin (aprox. -20 kcal/mol). Those values suggest the two former molecules to be good binders to $3CL^{Pro}$ and the latest to be somehow of lesser quality. When analyzing each monomer individually, the $\Delta G_{binding}$ values are consistent with the structural observation with Speciophylline having almost symmetric values (ca. -33 kcal/mol), and Cadambine and Proanthocyanidin having different magnitudes. The closer energy values for Cadambine and Speciophiline are consistent with the structural similarities between both alkaloids with respect to Proanthocyanidin.

Table 2. Ligand-protease $\Delta G_{binding}$ in kcal/mol. Average obtained from 250 frames for each MD trajectory (one per ns) using MM-GBSA method in AmberTools18. The following parameters were used: igb=2, saltcon=0.100.

	Cadambine	Proanthocyanidin B2	Speciophylline
Monomer B	-51.92 ± 6.03	-21.20 ± 6.22	-33.49 ± 4.88
Monomer A	-32.25 ± 5.84	-15.25 ± 7.31	-33.34 ± 6.15

In the light of the molecular dynamics analysis and the calculation of the free energy of binding, at least Cadambine and Speciophylline are predicted to present very good inhibition to the 2019-nCoV main protease main protease. Due to these components are found in ethanolic extract of Cat's claw may position itself as possible therapeutic herbal for COVID-19.

Preprints (www.preprints.org) | NOT PEER-REVIEWED | Posted: 28 June 2020 doi:10.20944/preprints202006.0326.v1

3.5. *Calculation of drug-likeness indices and scoring*

Calculated human pharmacokinetics profiles play a critical role in assessing the quality of novel anti-viral candidates. Early predictions of pharmacokinetic behavior of the promising antiviral compounds based on its structure could help finding safer and effectiveness leads for preclinical antiviral testing. Herein, we calculated and analyzed various drug-likeness indices for the most qualified Cat´s claw components (Table 3). Ten pharmacokinetics parameters were calculated as drug-likeness filter for Speciophylline, Cadambine, Proanthocyanidin B2 and compared to those N3 and three selected antiviral drugs. Results obtained demonstrate the feasibility of adequately of the selected components from Cat´s claw exhibiting suitable drug-like characteristics.

Table 3. Calculated drug-likeness properties for the most qualified Cat´s claw components.

Compound	M.W [a]	PSA [b]	n-Rot Bond (0-10)	n-ON (<10) [c]	n-OHNH [d]	Log $P_{o/w}$ [e]	LogK_{HSA} [f]	Caco-2 [g] (nm/s)	App. MDCK (nm/s) [h]	% HIA [i]	Lipinski Rule of five (≤1)
Speciophylline	368.432	82.804	1	8	1	1.709	-0.044	307	153	81	0
Cadambine	544.557	158.806	8	11	5	0.037	-0.592	27	11	27	0
Proanthocyanidin B2	578.528	209.177	10	12	10	0.505	-0.300	1	1	<25	1
N3	680.800	221.219	17	14	3	2.578	-0.497	6	11	85	2
Remdesivir[j]	602.583	196.086	16	16	5	1.135	-0.685	37	14	36	2
Ritonavir[j]	720.943	139.542	18	11	3	6.335	0.638	647	1014	75	2
Lopinavir[j]	628.810	124.690	16	9	4	5.751	0.554	510	598	83	2

[a] Molecular weight of the hybrid (150-500). [b] Polar surface area (PSA) (7.0–200 Å2). [c] n-ON number of hydrogen bond acceptors <10. [d] n-OHNH number of hydrogens bonds donors ≤5. [e] Octanol water partition coefficient (log Po/w) (–2.0 to 6.5). [f] Binding-serum albumin (KHSA) (-1.5 to 1.5). [g] Human intestinal permeation (<25 poor,>500 great). [h] Madin-Darby canine kidney (MDCK) cells permeation. [i] Human intestinal absorption (% HIA) (>80% is high, <25% is poor). [j] FDA-approved antiviral drugs used as references.

In addition, lipophilicity (calculated as Log $P_{o/w}$) is the key physicochemical property for rational drug design. This parameter provides valuable information about transport through lipid bilayers. Compounds that display high Log $P_{o/w}$ tend to have good

Preprints (www.preprints.org) | NOT PEER-REVIEWED | Posted: 28 June 2020 doi:10.20944/preprints202006.0326.v1

permeability across the cell wall [66, 67]. In this study, the selected compounds exhibited optimal $LogP_{o/w}$ values <6.5, notably Speciophylline has a $LogP_{o/w}$ of 1.709 (optimal value compared to 95% of current drugs) implying good permeability across the cell membrane of infected cells. Furthermore, the in silico passive transmembrane permeation was calculated for all compounds using Caco-2 cell monolayers or MDCK cells as model. Cadambine and Proanthocyanidin B2 exhibit low values of permeability (<27 nm/s), clearly suggesting poor bioavailability. However, an optimal value for the alkaloid Speciophylline was predicted (307 nm/s for Caco-2 model) close to Ritonavir and Lopinavir drugs and much better than inhibitor N3 (6 nm/s for Caco-2 model).

Finally, binding to serum albumin (expressed as $logK_{HSA}$) is the most important parameter for distribution and transport of antiviral drugs in the systemic circulation. Early prediction of this parameter reduces the amount of wasted time and resources for drug development candidates in the anti-viral therapy and management. Behavior of the selected compounds with human plasma protein ($LogK_{HSA}$) are within recommended values range (ranging from -0.30 to -0.044) compared to reference value taken from 95% of currently known drugs (Log K_{HSA} from -1.5 to 2.0). Optimal physicochemical properties obtained for the active components of Cat´s claw indicated that this herbal should be considered for the rapid progression in the antiviral treatment.

4. Conclusions

The coronavirus pandemic is a serious public health crisis due to high mortality, high basic reproduction numbers and neither approved drugs nor vaccines. The recent publication of the crystal structure of the 2019-nCoV main protease has provided the community with critical structural information. Potential inhibitors of this enzyme could have a major contribution in the reduction, prevention or eradication of the viral load of patients.

This study aimed at computationally explore if *Uncaria tomentosa* (Cat`s claw), an indigenous medicinal herb known for its anti-viral properties against other high mortality

 doi:10.20944/preprints202006.0326.v1

viruses, contains phytochemicals potentially able to inhibit the 2019-nCoV main protease, $3CL^{Pro}$.

After screening 26 key compounds of *Uncaria tomentosa* against the $3CL^{Pro}$ cleavage site, nine compounds displayed lower binding energies than those of known inhibitors of this enzyme (N3 as well as three FDA-approved antiviral drugs). Amongst those nine compounds, one of each family of well characterized active phytochemical fractions of Cat`s claw, namely Speciophylline, Cadambine and Proanthocyanidin B2, attracted our attention because of their strong docking scores (-8.1, -8.6 and -9.2 kcal/mol, respectively). The potential inhibitory effects of those molecules were further analyzed by means of ligand pathway simulations (which show very low barriers for binding), molecular dynamics of the docked complexes (until convergence at aprox. 250ns) and MM-GBSA free energy binding energy calculations (with values range from ca. -50 kcal/mol to ca. -15 kcal/mol). Altogether, these results confirm that the three compounds, and more particularly the alkaloid ones, have good predicted inhibitory profiles. To further anticipate throughout computation the therapeutic behavior of ethanolic extract of Cat´s claw, several physicochemical and ADME-score indices were calculated based on these three active molecules and compared to standard ranges for 95% of marketed drugs. The returned values show optimal drug-like properties for Speciophylline, Cadambine and Proanthocyanidin B2.

Due to the remarkable presence of these compounds from the ethanolic Cat´s claw extract, we believe that this *in silico* study at least point at *Uncaria tomentosa* as a whole as an interesting herb opening novel therapeutically horizons for COVID-19 treatment. Based on our findings, we believe that Cat's claw should be taken into consideration in looking for COVID-19 treatments.

Author Contributions: Conceptualization, O.H.-C. and A.F.Y.; methodology, A.F.Y and J.-D.M.; software, A.F.Y.; J.-E.S.-A. and L.T.S; validation, W.C.G. and J.-D.M.; formal analysis, J.-D.M.; investigation, O.H.-C. and A.F.Y.; data curation, W.C.G.; writing and editing-original draft preparation, O.H.-C.; A.F.Y.; J.D.M. and J.-E.S.-A.; writing—review and

editing, A.F.Y.; L.T.S. and J.D.-M.; visualization, W.C.G.; supervision, A.F.Y. All authors have read and agreed to the published version of the manuscript.

Funding: JSA, LTS and JDM gratefully acknowledge the financial support from the Spanish MINECO (CTQ2017-87889-P).

Acknowledgments: We would like to thank Universidad de Antioquia, Universidad Nacional Mayor de San Marcos and Universitat Autònoma de Barcelona.

Conflicts of Interest: "The authors declare no conflict of interest."

Abbreviations

PCA	Principal Component Analysis
ADME	Absorption, distribution, metabolism and excretion
MD	Molecular Dynamics
FDA	Food and Drug Administration
TNFα	Tumor necrosis factor alpha
EsSalud	Seguro Social de Salud (In Spanish)
PDB	Protein Data Bank

References

1. Singhal: T. A Review of Coronavirus Disease-2019 (COVID-19). Indian J. Pediatr. 2020;87(4):281-286.
2. Chen YW, Yiu CB, Wong KY. Prediction of the SARS-CoV-2 (2019-nCoV) 3C-like protease (3CL pro) structure: virtual screening reveals velpatasvir, ledipasvir, and other drug repurposing candidates. F1000Res. 2020; 9:129.
3. Wang C, Horby-Peter W, Hayden-Frederick G, Gao-George F. A novel coronavirus outbreak of global health concern. The Lancet. 2020;395(10223):470–473.
4. Mourya DT, Yadav PD, Ullas PT, Bhardwaj SD, Sahay RR, Chadha MS, et al. Emerging/re-emerging viral diseases & new viruses on the Indian horizon. Indian J. Med. Res. 2019;149(4):447-467.

5. Williamson J, Ramirez R, Wingfield T. Health, healthcare access, and use of traditional versus modern medicine in remote Peruvian Amazon communities: a descriptive study of knowledge, attitudes, and practices. Am. J. Trop. Med. Hyg. 2015;92(4):857-864.
6. Bussmann RW, Malca-García G, Glenn A, Sharon D, Chait G, Díaz D, et al. Minimum inhibitory concentrations of medicinal plants used in Northern Peru as antibacterial remedies. J. Ethnopharmacol. 2010 8;132(1):101-8.
7. Rojas-Rojas, T, Bourdy G, Ruiz E, Cerapio JP, Pineau P, Gardon J, et al. Herbal Medicine Practices of Patients With Liver Cancer in Peru: A Comprehensive Study Toward Integrative Cancer Management. Integr. Cancer. Ther. 2018;17(1):52-64.
8. Ben-Shabat S, Yarmolinsky L, Porat D, Dahan A. Antiviral effect of phytochemicals from medicinal plants: Applications and drug delivery strategies. Drug Deliv. Transl. Res. 2020;10(2):354-367.
9. Heitzman ME, Neto CC, Winiarz E, Vaisberg AJ, Hammond GB. Ethnobotany, phytochemistry and pharmacology of Uncaria (Rubiaceae). Phytochemistry. 2005;66(1):5-29.
10. Allen-Hall L, Cano P, Arnason JT, Rojas R, Lock O, Lafrenie RM. Treatment of THP-1 cells with Uncaria tomentosa extracts differentially regulates the expression if IL-1beta and TNF-alpha. J. Ethnopharmacol. 2007;109(2):312-7.
11. Bussmann RW, Sharon D. Traditional medicinal plant use in Northern Peru: tracking two thousand years of healing culture. J. Ethnobiol. Ethnomed. 2006; 2:47.
12. Keplinger K, Laus G, Wurm M, Dierich MP, Teppner H. *Uncaria tomentosa* (Willd.) DC.--ethnomedicinal use and new pharmacological, toxicological and botanical results. J. Ethnopharmacol. 1999;64(1):23-34.
13. Gonzales GF, Aguilar J, Villar M. The World Summit of Harmonization on Traditional, Alternative and Complementary Medicine (TACM) in Lima, Peru. Evid. Based Complement Alternat. Med. 2010;7(2):271-5.
14. Navarro M, Arnaez E, Moreira I, Hurtado A, Monge D, Monagas M. Polyphenolic Composition and Antioxidant Activity of *Uncaria tomentosa* Commercial Bark Products. Antioxidants (Basel). 2019;8(9):339.

15. Navarro M, Zamora W, Quesada S, Azofeifa G, Alvarado D, Monagas M. Fractioning of Proanthocyanidins of *Uncaria tomentosa*. Composition and Structure-Bioactivity Relationship. Antioxidants (Basel). 2017;6(3):60.
16. Aquino R, De Simone F, Pizza C, Conti C, Stein ML. Plant metabolites. Structure and in vitro antiviral activity of quinovic acid glycosides from *Uncaria tomentosa* and *Guettarda platypoda*. J Nat Prod. 1989;52(4):679-85.
17. Reis SR, Valente LM, Sampaio AL, Siani AC, Gandini M, Azeredo EL.; et al. Immunomodulating and antiviral activities of *Uncaria tomentosa* on human monocytes infected with Dengue Virus-2. Int. Immunopharmacol. 2008;8(3):468-76.
18. Lima-Junior RS, Mello-Cda S, Siani AC, Valente LM, Kubelka CF. *Uncaria tomentosa* alkaloidal fraction reduces paracellular permeability, IL-8 and NS1 production on human microvascular endothelial cells infected with dengue virus. Nat. Prod. Commun. 2013;8(11):1547-50.
19. Caon T, Kaiser S, Feltrin C, de Carvalho A, Sincero TC, Ortega GG, et al. Antimutagenic and antiherpetic activities of different preparations from *Uncaria tomentosa* (cat's claw). Food Chem. Toxicol. 2014;66;30-35.
20. Williams JE. Review of antiviral and immunomodulating properties of plants of the Peruvian rainforest with a particular emphasis on Una de Gato and Sangre de Grado. Altern. Med. Rev. 2001;6(6):567-79.
21. Sandoval M, Charbonnet RM, Okuhama NN, Roberts J, Krenova Z, Trentacosti AM, et al. Cat's claw inhibits TNF alpha production and scavenges free radicals: role in cytoprotection. Free Radic. Biol. Med. 2000; 9(1):71-8.
22. López-Galera RM, Ribera-Pascuet E, Esteban-Mur JI, Montoro-Ronsano JB, Juárez-Giménez JC. Interaction between Cat's claw and protease inhibitors atazanavir, ritonavir and saquinavir. Eur. J. Clin. Pharmacol. 2008;64(12):1235-6.
23. Akesson Ch, Pero RW, Ivars FC-Med 100, a hot water extract of *Uncaria tomentosa*, prolongs lymphocyte survival in vivo. Phytomedicine. 2003;10(1):23-33.
24. Chen SL, Yu H, Luo HM, Wu Q, Li CF, Steinmetz A. Conservation and sustainable use of medicinal plants: problems, progress, and prospects. Chin Med. 2016; 11:37.

25. Prajapat M, Sarma P, Shekhar N, Avti P, Sinha S, Kaur H, et al. Drug targets for corona virus: A systematic review. Indian J. Pharmacol. 2020; 52(1): 56–65.
26. Wu C, Liu Y, Yang Y, Zhang P, Zhong W, Wang Y, et al. Analysis of therapeutic targets for SARS-CoV-2 and discovery of potential drugs by computational methods, Acta Pharm. Sin. B. 2020. Advance online publication. https://doi.org/10.1016/j.apsb.2020.02.008
27. Yang H, Xie W, Xue X, Yang K, Ma J, Liang W. Design of wide-spectrum inhibitors targeting coronavirus main proteases. PLoS Biol. 2005;3:e324.
28. Morris G M, Huey R, Lindstrom W, Sanner MF, Belew RK, Goodsell DS.; et al. J. Comput. Chem. 2009, 30, 2785-2791.
29. Senanayake SL. Drug repurposing strategies for COVID-19. Future Drug. Discov (e-pub a head of print)
30. Wang J. Fast Identification of Possible Drug Treatment of Coronavirus Disease -19 (COVID-19) Through Computational Drug Repurposing Study. ChemRxiv, 2020.
31. Elfiky AA. Anti-HCV, nucleotide inhibitors, repurposing against COVID-19. Life Sci. 2020; 248:117477.
32. Chu CM, Cheng VC, Hung IF, Wong MM, Chan KH, Chan KS et al. Role of lopinavir/ritonavir in the treatment of SARS: Initial virological and clinical findings. Thorax 2004;59(3):252–256.
33. Agostini ML, Andres EL, Sims AC, Graham RL, Sheahan TP, Lu X, et al. Coronavirus susceptibility to the antiviral remdesivir (GS-5734) is mediated by the viral polymerase and the proofreading exoribonuclease. MBio. 2018;9(2):1–15.
34. Wang M, Cao R, Zhang L, et al. Remdesivir and chloroquine effectively inhibit the recently emerged novel coronavirus (2019-nCoV) *in vitro.* Cell Res.2020; 30:269–271.
35. Irwin JJ, Sterling T, Mysinger MM, Bolstad ES, Coleman RG. ZINC: a free tool to discover chemistry for biology. J. Chem. Inf. Model. 2012: 52:1757–1768.
36. ChemAxon. MarvinSketch. ChemAxon, Budapest. 2018. (http://www.chemaxon.com)

37. Morris GM, Goodsell DS, Halliday RS, Huey R, Hart WE, Belew RK, et al. Automated Docking Using a Lamarckian. Genetic Algorithm and Empirical Binding Free Energy Function. J. Comput. Chem., 1998, 19, 1639-1662.35.
38. Trott O, Olson AJ. AutoDock Vina: improving the speed and accuracy of docking with a new scoring function, efficient optimization, and multithreading. J. Comput. Chem. 2010; 30;31(2):455-61.
39. González-Alemán R, Hernández-Castillo D, Caballero J, Montero-Cabrera LA. Quality Threshold Clustering of Molecular Dynamics: A Word of Caution. J. Chem. Inf. Model. 2020, 60, 467–472.
40. Berman HM, Westbrook J, Feng Z, Gilliland G, Bhat TN, Weissig H, et al. The Protein Data Bank; 2000; Vol. 28.
41. Pettersen EF, Goddard TD, Huang CC, Couch GS, Greenblatt DM, Meng EC, et al. UCSF Chimera - A visualization system for exploratory research and analysis. J. Comput. Chem. 2004, 25, 1605–1612.
42. Frisch MJ, Trucks GW, Schlegel HB, Scuseria GE, Robb GE, Cheeseman JR, et al. Gaussian 09, Revision D.01. Gaussian, Inc. Wallingford, CT, USA, 2009.
43. Bayly CI, Cieplak P, Cornell WD, Kollman PA. A well-behaved electrostatic potential based method using charge restraints for deriving atomic charges: The RESP model. J. Phys. Chem. 1993, 97, 10269–10280.
44. Case DA, Ben-Shalom IY, Brozell SR, Cerutti DS, Cheatham TE, Cruzeiro VWD, et al. Amber 2018. Univ. Calif. 2018.
45. Rodríguez-Guerra Pedregal J, Alonso-Cotchico L, Velasco-Carneros L, Maréchal J-D. OMMProtocol: A command line application to launch molecular dynamics simulations with OpenMM. ChemRxiv 2018.
46. Smith LJ, Daura X, Van Gunsteren WF. Assessing equilibration and convergence in biomolecular simulations. Proteins Struct. Funct. Genet. 2002.
47. Grossfield A, Zuckerman DM. Chapter 2 Quantifying Uncertainty and Sampling Quality in Biomolecular Simulations. Annu. Rep. Comput. Chem. 2009

48. Haider Z, Subhani MM, Farooq MA, Ishaq M, Khalid M, Khan RSA, et al. In silico discovery of novel inhibitors against main protease (Mpro0 of SARS-CoV-2 using pharmacophore and molecular docking based virtual screening from ZINC database. Preprints. (2020).
49. Khaerunnisa S, Kurniawan H, Awaluddin R, Suhartati, Soetjipto S. Potential Inhibitor of COVID-19 Main Protease (Mpro) From Several Medicinal Plant Compounds by Molecular Docking Study. Preprint. 2020, (https://www.preprints.org/manuscript/202003.0226/v1).
50. Chauhan, N. Possible Drug Candidates for COVID-19. ChemRxiv, 2020.
51. Kaifu G, Duy D, Rui N, Wei G. Machine intelligence design of 2019-nCoV drugs. BioRxiv. 2020.
52. Talluri, S. Virtual Screening based prediction of potential drugs for COVID-19. Preprints, 2020. (https://www.preprints.org/manuscript/202002.0418/v2).
53. Chang Y, Tung Y, Lee K, Chen T, Hsiao Y, Chang H, et al. Potential Therapeutic Agents for COVID-19 Based on the Analysis of Protease and RNA Polymerase Docking. Preprints 2020. https://www.preprints.org/manuscript/202002.0242/v1.
54. Yang ZF, Bai LP, Huang WB, Li XZ, Zhao SS, Zhong NS, et al. Comparison of in vitro antiviral activity of tea polyphenols against influenza A and B viruses and structure-activity relationship analysis. Fitoterapia. 2014, 93, 47-53.
55. Luganini A, Terlizzi ME, Catucci G, Gilardi G, Maffe ME, Gribaudo G. The Cranberry Extract Oximacro® Exerts in vitro Virucidal Activity Against Influenza Virus by Interfering with Hemagglutinin. Front. Microbiol. 2018, 7, 1826-1838.
56. Tsukuda S, Watashi K, Hojima T, Isogawa M, Iwamoto M, Omagari K, et al. A new class of hepatitis B and D virus entry inhibitors, proanthocyanidin and its analogs, that directly act on the viral large surface proteins. Hepatology. 2017, 65, 1104-1116.
57. Terlizzi ME, Occhipinti A, Luganini A, Maffei ME, Gribaudo G. Inhibition of herpes simplex type 1 and type 2 infections by Oximacro(®), a cranberry extract with a high content of A-type proanthocyanidins (PACs-A). Antiviral Res. 2016, 132, 154-164.

58. Lipson SM, Karalis G, Karthikeyan L, Ozen FS, Gordon RE, Ponnala S. et al. Mechanism of Anti-rotavirus Synergistic Activity by Epigallocatechin Gallate and a Proanthocyanidin-Containing Nutraceutical. Food Environ Virol. 2017, 9, 434-443.
59. Joshia S, Howell A, D'Souzaa D. Antiviral effects of blueberry proanthocyanidins against Aichi virus. Food Microbiol. 2019, 82, 202–208.
60. Sánchez-Aparicio JE, Sciortino G, Herrmannsdoerfer DV, Chueca PO, Pedregal JRG, Maréchal JD. GPathFinder: Identification of Ligand-Binding Pathways by a Multi-Objective Genetic Algorithm. Int. J. Mol. Sci. 2019, 20, 3155.
61. Komatsu TS, koyama YM, Okimoto N, Morimoto G, Ohno Y, Taiji M. COVID-19 related trajectory data of 10 microseconds all atom molecular dynamics simulation of SARS-CoV-2 dimeric main protease 2020. Mendeley Data, v1. http://dx.doi.org/10.17632/vpps4vhryg.1
62. Eastman P, Swails J, Chodera JD, McGibbon RT, Zhao Y, Beauchamp KA, Wang LP, Simmonett AC, Harrigan MP, Stern CD, et al. OpenMM 7: Rapid development of high performance algorithms for molecular dynamics. PLoS Comput. Biol. 2017, 13, 1–17.
63. Hornak V, Abel R, Okur A, Strockbine B, Roitberg A, Simmerling C. Comparison of multiple amber force fields and development of improved protein backbone parameters. Proteins 2006, 65, 712–725.
64. Sciortino G, Sanchez-Aparicio JE, Pedregal JRG, Garribba E, Maréchal JD. Computational insight into the interaction of oxaliplatin with insulin Metallomics 2019 11, 765-773
65. Alonso-Cotchico L, Pedregal JRG, Lledós A, Maréchal JD. The Effect of Cofactor Binding on the Conformational Plasticity of the Biological Receptors in Artificial Metalloenzymes: The Case Study of LmrR Front. Chem. 2019, 7, 211
66. Ertl P, Rohde B, Selzer P. Fast Calculation of Molecular Polar Surface Area as a Sum of Fragment-Based Contributions and Its Application to the Prediction of Drug Transport Properties. J. Med. Chem. 2000, 42, 3714–3717.

 doi:10.20944/preprints202006.0326.v1

67. Lipinski CA, Lombardo F, Dominy BW, Feeney PJ. Experimental and computational approaches to estimate solubility and permeability in drug discovery and development settings. Adv. Drug. Deliv. Rev. 1997, 23, 3-25.